Evaluating the Role of Re-adsorption of Dissolved Hg^{2+} during Cinnabar Dissolution Using Isotope Tracer Technique

Journal:	*Environmental Science & Technology*
Manuscript ID	es-2015-046629
Manuscript Type:	Article
Date Submitted by the Author:	23-Sep-2015
Complete List of Authors:	Jiang, Ping; Florida International University, Department of Chemistry & Biochemistry Li, Yanbin; Ocean University of China , Key Laboratory of Marine Chemistry Theory and Technology, Ministry of Education Liu, Guangliang; Florida International University, Chemistry & Biochemistry/SE Env Res Ctr Yang, GuiDi; Fujian Agriculture and Forestry University Lagos, Leonel; Florida International University, Applied Research Center Yin, Yongguang; Research Center for Eco-Environmental Sciences, Chinese Academy of Sciences, Gu, Baohua; Oak Ridge National Laboratory, Environmental Sciences Division Jiang, Guibin; Chinese Academy of Sciences, Research Ctr. Eco-Environmental Sciences Cai, Yong; Florida International University, Department of Chemistry & Biochemistry

Evaluating the Role of Re-adsorption of Dissolved Hg^{2+} during Cinnabar Dissolution Using Isotope Tracer Technique

Ping Jiang[1‡], Yanbin Li[1∆], Guangliang Liu[‡†], Guidi Yang[‖], Leonel Lagos[‡], Yongguang Yin[§], Baohua Gu[|], Guibin Jiang[§], and Yong Cai*[‡†]

[‡]Department of Chemistry and Biochemistry, Florida International University, Miami, FL 33199, USA

[†]Southeast Environmental Research Center, Florida International University, Miami, FL 33199, USA

[∆]Key Laboratory of Marine Chemistry Theory and Technology, Ministry of Education/Qingdao Collaborative Innovation Center of Marine Science and Technology and College of Chemistry and Chemical Engineering, Ocean University of China, Qingdao, 266100, China

[‡] Applied Research Center, Florida International University, Miami, FL 33199, USA

[§]State Key Laboratory of Environmental Chemistry and Ecotoxicology, Research Center for Eco-Environmental Sciences, Chinese Academy of Sciences, Beijing, 100085, China

[‖]College of Life Sciences, Fujian Agriculture and Forestry University, Fuzhou, 350002, China

[|]Environmental Sciences Division, Oak Ridge National Laboratory, Oak Ridge TN 37831, USA

***Corresponding author:**

Yong Cai

Tel: 305-348-6210

Fax: 305-348-3772

Email address: cai@fiu.edu

[1]These authors contributed equally to this work.

TOC

Cinnabar Dissolution and Readsorption of Hg^{2+}

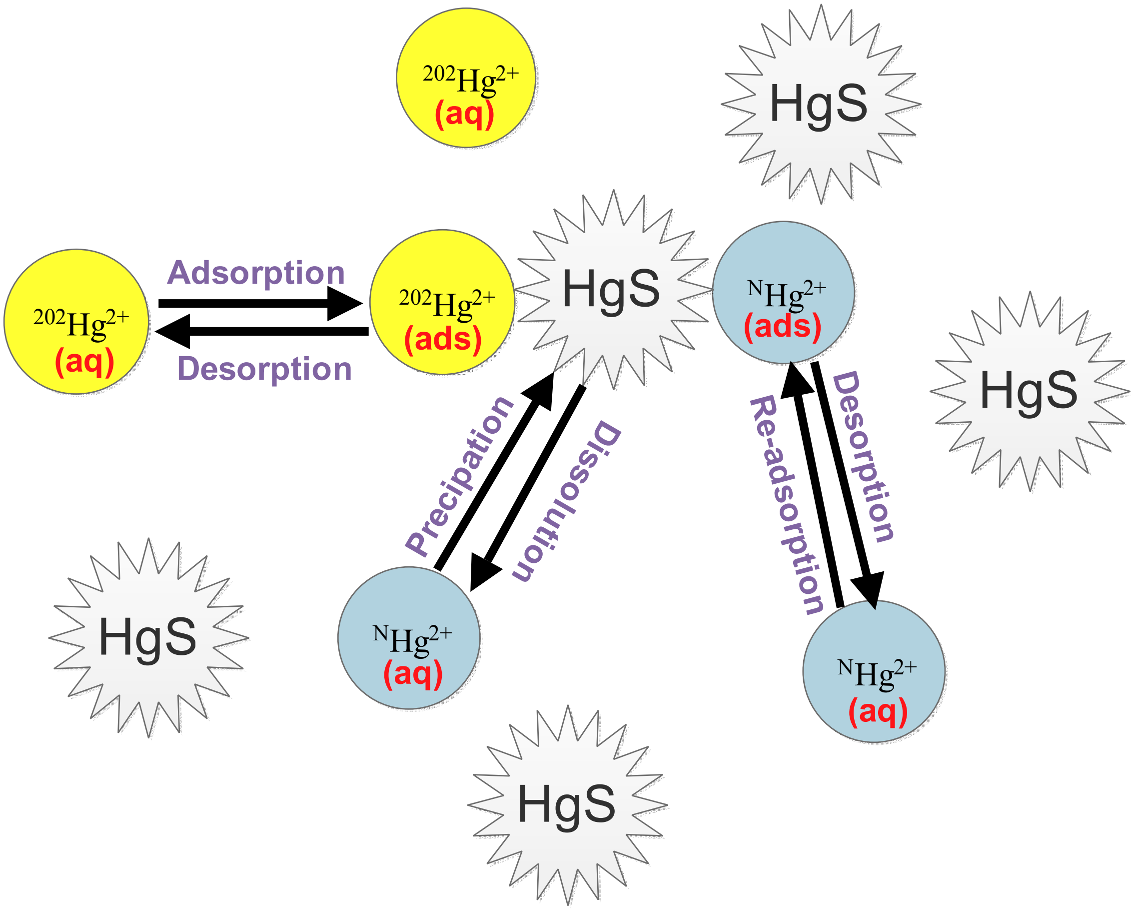

$\mathbf{^{N}Hg^{2+}}$**(aq)** is the released Hg from cinnabar present in the aqueous phase.
$\mathbf{^{N}Hg^{2+}}$**(ads)** is the released Hg re-adsorbed on cinnabar surface.
$\mathbf{^{202}Hg^{2+}}$ **(aq)** is spiked $^{202}Hg^{2+}$ present in the aqueous phase.
$\mathbf{^{202}Hg^{2+}}$ $^{+}$**(ads)** is spiked $^{202}Hg^{2+}$ adsorbed on cinnabar surface.

ABSTRACT

Cinnabar dissolution is an important factor controlling mercury (Hg) cycling as this process makes the originally stable Hg more reactive and bioavailable, increasing the possibility of Hg transport, methylation and bioaccumulation in aquatic environments. Recent studies have suggested the co-occurrence of released Hg re-adsorption during the course of cinnabar dissolution. However, this process has neither been quantitatively assessed nor taken into account when measuring cinnabar dissolution rate, mainly due to the lack of a feasible technique that can differentiate the dissolution and re-adsorption processes. The lack of the quantification of re-adsorption could result in insufficient evaluation of the importance of cinnabar dissolution. In this study, a new method, based on isotope tracing ($^{202}Hg^{2+}$) and isotope dilution ($^{199}Hg^{2+}$) techniques, was developed to decipher the role of re-adsorption of released Hg in estimating cinnabar dissolution. The developed method includes two key components: 1) accurate measurement of both Hg released from cinnabar and the spiked $^{202}Hg^{2+}$ in aqueous phase and 2) estimation of re-adsorbed Hg on cinnabar surface via the reduction in the amount of spiked $^{202}Hg^{2+}$. Finally, the developed method was applied to investigate cinnabar dissolution and re-adsorption of released Hg under both aerobic and anaerobic conditions. The results showed that the released Hg for trials purging with oxygen could reach several hundred μg L^{-1} while no significant dissolution of cinnabar was detected under anaerobic condition. Spiked $^{202}Hg^{2+}$ was observed to be adsorbed on the cinnabar surface rapidly, supporting the observation of co-occurrence of re-adsorption during cinnabar dissolution. Cinnabar dissolution rate with the consideration of Hg re-adsorption using the newly developed method (0.0208 h^{-1}) was estimated to be much higher (~2 times) than that calculated with the Hg detected alone in the aqueous phase (0.0109 h^{-1}). Results of this study suggest that ignoring the re-adsorption of Hg on cinnabar surface can significantly underestimate

the importance of cinnabar dissolution, highlighting the necessity of applying the developed method in future cinnabar dissolution studies.

INTRODUCTION

Cinnabar (HgS), a major ore mineral, is one of the largest mercury (Hg) sinks in contaminated sediments and soils.[1] It has been considered as the most insoluble and least leachable Hg species due to its low solubility product constant ($k_{sp} = 10^{-55.9 \sim -50.9}$).[2] The formation of cinnabar in the environment plays a major role in restraining Hg biogeochemical cycling. However, previous studies showed that cinnabar can also serve as a continuous source of inorganic Hg in natural environment due to the fact that a variety of environmental factors can facilitate the dissolution of cinnabar. These factors include the presence of iron(III) in acidic water,[3] sulfide in water,[4] and dissolved organic matter (DOM).[5-7] The enhanced dissolution of cinnabar could be an important process controlling Hg cycling in aquatic environments as this process would make the originally stable Hg more reactive and bioavailable, increasing the possibility of Hg transport, methylation and bioaccumulation, posing a great risk to humans and wildlife. This process is particularly important at areas where soils and sediments are heavily contaminated with Hg since even the release of a small fraction of sequestered Hg would remarkably increase the amount of Hg available in aquatic environment.[8]

Dissolution of cinnabar in aquatic environment is very complex and the process could be conceptually simplified in two steps, 1) elimination of dissolution products (S^{2-} and Hg^{2+}) in the aqueous phase and 2) the subsequent dissolution of cinnabar (Table S1, Figure S1).[2, 9, 10] A variety of environmental factors are expected to enhance or inhibit cinnabar dissolution via affecting the fate of cinnabar dissolution products. These factors include pH, redox potential (Eh), and Hg binding ligands.[3, 6, 11, 12] Sulfide (S^{2-}), one of the cinnabar dissolution products, could be eliminated from the system via oxidation to SO_4^{2-} under aerobic condition at pH 5-8 [3, 10, 12-14] or conversion to HS^- and H_2S under anaerobic condition.[2] The former pathway may play a more important role as quicker dissolution of cinnabar was observed in the presence of O_2.[3, 10, 11] Hg^{2+}, the other product, could bind with organic ligands, in particular thiol-containing moieties in dissolved organic matter (DOM).[6, 9, 15] The binding process is expected to reduce the amount of free Hg^{2+} in aqueous phase and thus enhance cinnabar dissolution. Contrary results were sometimes observed regarding the effects of organic ligands on cinnabar dissolution. For instance, minor changes in cinnabar dissolution were observed in the presence and absence of organic ligands (salicylic acid, acetic acid, EDTA, or cysteine).[5-7, 14] These inconsistent results were speculated to be attributed to the differences in binding strength between those ligands and Hg and the possible re-adsorption of released Hg on cinnabar.[6]

Hg^{2+} ion can be adsorbed on a variety of solid phases in natural environments, e.g., particles in water,[16] soil,[17] sediment[18] and minerals[19]. The adsorption process may involve one or several possible mechanisms, including physisorption (Van der Waals interaction) and chemisorptions (ion exchange or surface complexation). Surface complexation was considered to be the possible mechanism of Hg^{2+} ions adsorption on HgS in most studies.[10, 20] Surface of cinnabar (with a pH_{pzc} of 3-4) is expected to be negatively charged in natural aquatic environments with a pH of 6-8 due to the deprotonation of exposed sulfhydryl groups.[6, 21] Since the dominant dissolved Hg(II) species in aquatic environments are often uncharged complexes, inorganic or organic complex formation, ion exchange should not be the major mechanism of Hg adsorption on cinnabar.[22] Experimental results have provided both direct and indirect evidences for the occurrence of Hg re-adsorption on cinnabar surface.[6, 10, 11, 13] For instance, the amount of Hg released was found to be much lower than that of S (normally represented by SO_4^{2-}), in strong disagreement with the stoichiometric estimation, indicating the adsorption of released Hg back on cinnabar particles.[6] Hg^{2+} added into cinnabar suspension were observed to decrease quickly, further proving the occurrence of this process.[10] Nevertheless, this process has not yet been taken into account when measuring cinnabar dissolution rate in previous studies,[6, 7, 10, 11, 14] mainly due to the lack of a feasible technique that can differentiate the dissolution and re-adsorption processes. It is almost impossible to determine the re-adsorption rate of released Hg on cinnabar using traditional Hg addition method in consideration of the simultaneous dissolution of Hg from cinnabar. Hg adsorbed on cinnabar is expected to be very different in comparison with that of HgS in their environmental behavior, therefore, resulting in insufficient evaluation of the importance of cinnabar dissolution in the environment.

Mercury isotope tracer technique has been widely applied in studying transport and transformation of Hg (e.g., methylation/demethylation and oxidation/reduction[23, 24]) in recent years mainly due to the virtues of high precision and ability of simultaneously determining the rates of multiple processes. It has also been successfully used to quantify the adsorption and desorption of Hg in sediments.[18] The objective of this study was to decipher the role of re-adsorption of the dissolved Hg in cinnabar dissolution. It is expected that the application of isotope tracer technique would make it feasible to simultaneously differentiate the dissolution and re-adsorption processes. An experimental approach, using both isotope tracing and isotope dilution techniques, was developed to monitor Hg released into the solution as well as Hg re-adsorbed on cinnabar during the course of cinnabar dissolution. Equations were then derived to calculate the rates of cinnabar dissolution and Hg re-adsorption. The major virtue of the developed method is its ability to decipher the re-adsorption of released Hg on cinnabar during cinnabar dissolution. This method was then applied to investigate the dissolution of cinnabar and re-adsorption of released Hg under both aerobic and anaerobic conditions.

MATERIALS AND METHODS

Reagents

^{202}Hg metal (^{202}Hg(0), 99.20%) was purchased from Cambridge Isotope Laboratories (Andover, MA). Enriched ^{201}HgO (atomic percentage, 96.17 ± 0.56%) and ^{199}HgO (atomic percentage, 91.09 ±0.05%) were from Oak Ridge National Laboratory (Oak Ridge, Tennessee). $^{202}Hg(NO_3)_2$ (measured atomic percentage, 99.70%) was prepared by dissolving ^{202}Hg metal in concentrated HNO_3, while $^{201}HgCl_2$ (measured atomic percentage, 96.17%) and $^{199}HgCl_2$ solution (measured atomic percentage, 90.66%) were prepared by dissolving ^{201}HgO and ^{199}HgO in 10% HCl (v/v). Cinnabar (HgS, 99%) was purchased from Sigma-Aldrich. Concentrated nitric acid and hydrochloric acid were trace metal grade (Fisher Scientific). Stannous chloride ($SnCl_2 \cdot 2H_2O$, 99.2%) and other chemicals were all reagent grade or higher (Fisher Scientific). Argon, nitrogen and oxygen (ultra high purity) were purchased from Airgas. $NaNO_3/NaOH$ solution was prepared by adding 0.01mol L^{-1} NaOH into 10 μmol L^{-1} HNO_3 solution until achieving pH 8.0.

Pretreatment of cinnabar and selection of filters

The surface of cinnabar was cleaned prior to use by soaking and shaking the cinnabar powder (0.02 g) in 1 mol L^{-1} HNO_3 at 150 rpm (Orbital shaker, Henry Troemner LLC) for 3 days and subsequently filtering though a 0.45 μm PVDF membrane (Millipore).[7] Cinnabar on the filter membrane was washed until the filtrate reaching neutral using approximately 2.5 L DI (de-ionized) water (>18.2 MΩ) and then transferred to a 250 mL Teflon bottle containing 200 mL $NaNO_3/NaOH$ solution (pH 8.0). The final concentration of cinnabar in the suspension was approximately 100 mg L^{-1} as HgS. The average size of cinnabar was approximately 3,272 nm determined by dynamic light scattering (DLS) (Malvern Zetasizer Nano-ZS, Westborough, MA) (Supporting Information Fig. S2). DI water and $NaNO_3/NaOH$ solution used were purged overnight with N_2 to eliminate O_2. All procedures were performed in a N_2 glove box to avoid the exposure to air. Experiments were conducted to examine the adsorption of Hg on four types of filters (0.22 μm PTFE, 0.45 μm PTFE, 0.22 μm PVDF, and 0.45 μm PVDF). 0.22 μm PTFE filter was chosen in this study since it had the best recovery for Hg with minimum adsorption on the filter (Supporting Information, Table S2).

Simultaneous determination of cinnabar dissolution and Hg^{2+} re-adsorption in the presence of N_2 and O_2

Experiments using isotope tracer were designed to monitor the adsorption of Hg^{2+} on cinnabar during the course of cinnabar dissolution experiments. $^{202}HgNO_3$ (215 µL, 46.6 mg L^{-1} as Hg) was spiked into a 250 mL Teflon bottle with 180 mL $NaNO_3$/NaOH solution. Pretreated cinnabar (0.02 g wt.) was then added into the solution. The volume of the suspension solution was adjusted to 200 mL by adding $NaNO_3$/NaOH solution. The final concentrations of $^{202}Hg^{2+}$ and cinnabar were 50 µg L^{-1} as Hg and 100 mg L^{-1} as HgS, respectively. After shaking vigorously, 2.5 mL suspension was immediately sampled from each bottle using a 2.5 mL syringe and filtered through a 0.22 µm PTFE membrane (representing time 0). Bottles with the remaining suspensions were then shaken at 125 rpm with the purging of N_2 (~55 mL min^{-1}, treatment 1) or O_2 (~55 mL min^{-1}, treatment 2). Triplicates (three independent Teflon bottles) were prepared for each treatment. An aliquot of suspension (2.5 mL) was sampled from each bottle at 1, 2, 4, 6, 8, 10, 23, 30, 47, and 54 h, respectively, then filtered and preserved in a 4 ^{o}C refrigerator prior to analysis. Dissolved ^{201}Hg and ^{202}Hg in the filtrates were analyzed using an isotope dilution method. Upon analysis, 44.2 µL $^{199}HgCl_2$ (453 µg L^{-1} Hg) was spiked into 2 mL filtrate, mixed thoroughly, diluted to 20 mL and then stabilized for 1 hour. $^{199}Hg^{2+}$, $^{201}Hg^{2+}$ and $^{202}Hg^{2+}$ in the solutions were detected by a flow injection mercury analysis system (FIAS, from PerkinElmer) coupled with inductively coupled plasma mass spectrometry (ICP-MS, Elan DRC-e from PerkinElmer) following the method of isotope dilution technique.[25] Details can be found in the

Supporting Information. Concentrations of spiked $^{202}Hg^{2+}$ and Hg^{2+} released from the HgS in the aqueous phase were calculated, as detailed below in Results and Discussion section.

Thermodynamics of Hg adsorption on cinnabar

Thermodynamic experiments were further conducted to evaluate the adsorption capacity of Hg^{2+} on cinnabar. Adsorption of spiked $^{202}Hg^{2+}$ on cinnabar was observed to achieve equilibrium after 6 hours according to the results of preliminary experiments. The procedures for the adsorption experiments used here were identical to treatment 1 of the above experiment (purging with N_2). $^{202}Hg^{2+}$ was spiked into the cinnabar suspension at the final concentrations of 0, 10, 20, 50, 100, 200, and 400 μg L^{-1}. After shaking the bottles at 125 rpm for 6 hours, 2.5 mL sample was collected from each bottle, filtered through a 0.22 μm PTFE membrane, and stored at 4°C for analysis. Concentrations of the spiked $^{202}Hg^{2+}$ were then analyzed using the aforementioned isotope dilution method.

Data analysis

Calculation of parameters relevant to the thermodynamics of Hg adsorption on cinnabar

Langmuir (Eq. (1)) and Freundlich isotherms (Eq. (2))[26-32] were the two most commonly used adsorption isotherm equations which have been utilized to describe the adsorption of metal ions (including Hg) on solid adsorbents. Both models were adopted here to calculate the thermodynamic adsorption parameters of Hg adsorption on cinnabar. Nonlinear regression of q_e against C_e was conducted using OriginPro 8 (OriginLab) to calculate the parameters related to the Hg adsorption on cinnabar (q_m and K_L, K_F and n).

$$q_\mathrm{e} = \frac{q_\mathrm{m} k_\mathrm{L} C_\mathrm{e}}{1 + k_\mathrm{L} C_\mathrm{e}} \quad (1)$$

$$q_\mathrm{e} = K_\mathrm{F} C_\mathrm{e}^{1/\mathrm{n}} \quad (2)$$

where q_e is the adsorption capacity at equilibrium (µg g^{-1}), q_m is the maximum monolayer adsorption capacity (µg g^{-1}), K_L is the Langmuir constant (L µg^{-1}), C_e is the concentration of residue ^{202}Hg ions in the solution after equilibrium (µg L^{-1}), K_F is the Freundlich adsorption capacity constant (µg g^{-1}), n is the Freundlich constant related to the surface heterogeneity.

Calculation of parameters relevant to the kinetic adsorption of Hg on cinnabar and kinetic dissolution of cinnabar

The kinetic adsorption of Hg^{2+} on cinnabar can be described as a pseudo-second order reaction (Eq. (3))[33] while first order reaction (Eq. (4))[34] has been previously used to describe cinnabar dissolution. These models were selected and tested in this study. By integrating Eq. (3) and (4), variations in q_t and C with time can be described as Eq. (5) and (6), respectively. Nonlinear regression was conducted to calculate the adsorption rate constants (K_2) and dissolution rate constant of cinnabar (k).

$$\frac{dq_t}{dt} = k_2(q_e - q_t)^2 \quad (3)$$

$$\frac{dC}{dt} = k(C_0 - C) \quad (4)$$

$$\frac{t}{q_t} = \frac{1}{K_2 {q_e}^2} + \frac{1}{q_e} t \quad (5)$$

$$C = C_0 . (1 - e^{-kt}) \quad (6)$$

where q_t is the adsorption capacity at time t (µg g^{-1}), K_2 is the adsorption rate constant (g µg^{-1} h^{-1}), C_0 is the concentration of released Hg after equilibrium (µg L^{-1}), C is the concentration of released Hg at time t (µg L^{-1}), and k is the apparent dissolution rate constant (hour $^{-1}$).

RESULTS AND DISCUSSION

Developing a method for simultaneously monitoring Hg adsorption and dissolution using isotope dilution and isotope tracer technique

A portion of the released Hg can be re-adsorbed on cinnabar surface after dissolving from cinnabar particle, resulting in the coexistence of two forms of Hg in the cinnabar suspension, the released Hg present in the aqueous phase and released Hg re-adsorbed on cinnabar surface (Fig. 1). Concentration of the released Hg present in the aqueous phase can be determined readily, whereas it is still a challenge to directly measure the released Hg re-adsorbed on cinnabar surface. Without considering Hg re-adsorption can result in underestimation in Hg dissolution rate since only a portion of the released Hg (in the aqueous phase) is counted. To quantify the sum of Hg released from cinnabar (in the aqueous phase and re-adsorbed on cinnabar surface), a new method based on isotope tracer technique was developed. The rationale is that re-adsorbed Hg on cinnabar surface ($^{N}Hg^{2+}$(ads)) can be estimated by decreased amounts of the spiked isotope-enriched Hg ($^{202}Hg^{2+}$(aq)) in aqueous phase. Developing such a method includes two key steps: 1) measuring both released Hg in the aqueous phase ($^{N}Hg^{2+}$(aq)) and the residual $^{202}Hg^{2+}$ ($^{202}Hg^{2+}$(aq)) in the aqueous phase, and 2) developing an approach that can estimate re-adsorbed Hg on cinnabar surface ($^{N}Hg^{2+}$(ads)) by the reducing amount of spiked $^{202}Hg^{2+}$ in the aqueous phase ($^{202}Hg^{2+}$(aq)).

Hg isotopes in the filtrate were analyzed using isotope dilution technique. Prior to analyzing the samples, a known amount of $^{199}Hg^{2+}$ was spiked into the filtrate to serve as an internal standard. Abundances of $^{202}Hg^{2+}$, $^{199}Hg^{2+}$, and $^{201}Hg^{2+}$ (N_{202}, N_{199}, N_{201}) in the final solution were analyzed and the ratios of $^{201}Hg/^{199}Hg$ and $^{202}Hg/^{199}Hg$ (R_{199}^{201} and R_{199}^{202}) were determined. Hg isotope ratios in the filtrates were different from the natural abundance of Hg because of the addition of $^{202}Hg^{2+}$ at zero time. These isotope ratios also changed over time accompanying Hg dissolution from cinnabar and adsorption of the spiked $^{202}Hg^{2+}$. Therefore, traditional isotope dilution method for analyzing samples with the natural abundance of Hg isotopes[35-39] is not applicable here for calculating Hg concentrations in the filtrates. A new method was developed in order to simultaneously calculate Hg originated from cinnabar dissolution and residual spiked $^{202}Hg^{2+}$ in the filtrates.

Since all 7 natural Hg isotopes were present in the used isotope-enriched Hg ($^{202}Hg^{2+}$ and $^{199}Hg^{2+}$) because of impurities contained, Hg isotopes in the final filtrates originated from three sources, including cinnabar dissolution (with natural abundance of Hg isotopes, $C_d(aq)$), spiked $^{202}Hg^{2+}$ ($C_x(aq)$), and added $^{199}Hg^{2+}$ ($C_y(aq)$). In consideration of all these sources, the ratios of $^{201}Hg/^{199}Hg$ (R_{199}^{201}) and $^{202}Hg/^{199}Hg$ (R_{199}^{202}) can be described using the following functions (Eq. (7)-(8)):

$$R_1 = R_{199}^{201} = \frac{N_{201}}{N_{199}} = \frac{C_\mathrm{d}(\mathrm{aq})\,A_\mathrm{n}^{201} + C_\mathrm{x}(\mathrm{aq})A_{202}^{201} + C_\mathrm{y}(\mathrm{aq})A_{199}^{201}}{C_\mathrm{d}(\mathrm{aq})A_\mathrm{n}^{199} + C_\mathrm{x}(\mathrm{aq})A_{202}^{199} + C_\mathrm{y}(\mathrm{aq})A_{199}^{199}} \qquad (7)$$

$$R_2 = R_{199}^{202} = \frac{N_{202}}{N_{199}} = \frac{C_\mathrm{d}(\mathrm{aq})A_\mathrm{n}^{202} + C_\mathrm{x}(\mathrm{aq})A_{202}^{202} + C_\mathrm{y}(\mathrm{aq})A_{199}^{202}}{C_\mathrm{d}(\mathrm{aq})A_\mathrm{n}^{199} + C_\mathrm{x}(\mathrm{aq})A_{202}^{199} + C_\mathrm{y}(\mathrm{aq})A_{199}^{199}} \qquad (8)$$

where R_{199}^{201} represents the ratio of ^{201}Hg to ^{199}Hg in the final solution; R_{199}^{202} represents the ratio of ^{202}Hg to ^{199}Hg in the final solution; $C_d(aq)$(μg L^{-1}) represents the concentration of natural Hg (from HgS dissolution) in the solution; $C_x(aq)$ (μg L^{-1}) represents the residual concentration of spiked ^{202}Hg in the solution; $C_y(aq)$ (μg L^{-1}) represents the concentration of ^{199}Hg added after filtration in the solution; A_n^i represents the abundance of i isotope of Hg in natural Hg; A_{202}^i represents the abundance of i isotope Hg in spiked ^{202}Hg-enriched Hg; A_{199}^{i} represents the abundance of i isotope Hg in the used ^{199}Hg-enriched Hg.

By solving Eq. (7) and Eq. (8), the concentrations of released Hg present in the aqueous phase $C_d(aq)$ and residual spiked ^{202}Hg $C_x(aq)$ in the solution can be calculated by Eqs. (9) and (10), respectively. This isotope dilution method provides a precise tool to determine the concentrations of both released Hg and residual spiked $^{202}Hg^{2+}$ in the filtrates (C_d (aq) and C_x (aq)) at each sampling time of the dissolution experiment. Both

$C_{\mathrm{d}}(\mathrm{aq})$ and $C_{\mathrm{x}}(\mathrm{aq})$ are necessary for the later calculation of cinnabar dissolution rate and re-adsorption rate of released Hg.

$$C_{\mathrm{x}} = \frac{R_1 C_{\mathrm{y}}(\mathrm{aq})(A_{\mathrm{n}}^{199} A_{199}^{202} - A_{\mathrm{n}}^{202} A_{199}^{199}) + R_2 C_{\mathrm{y}}(\mathrm{aq})(A_{\mathrm{n}}^{201} A_{199}^{199} - A_{\mathrm{n}}^{199} A_{199}^{202}) + C_{\mathrm{y}}(\mathrm{aq})(A_{\mathrm{n}}^{202} A_{199}^{201} - A_{\mathrm{n}}^{201} A_{199}^{202})}{R_1(A_{\mathrm{n}}^{202} A_{202}^{199} - A_{\mathrm{n}}^{199} A_{202}^{202}) + R_2(A_{\mathrm{n}}^{199} A_{202}^{201} - A_{\mathrm{n}}^{201} A_{202}^{199}) + (A_{\mathrm{n}}^{201} A_{202}^{202} - A_{\mathrm{n}}^{202} A_{202}^{201})} \quad (9)$$

$$C_{\mathrm{d}} = \frac{R_1 C_{\mathrm{y}}(\mathrm{aq})(A_{199}^{199} A_{202}^{202} - A_{202}^{199} A_{199}^{202}) + R_2 C_{\mathrm{y}}(\mathrm{aq})(A_{199}^{201} A_{202}^{199} - A_{202}^{201} A_{199}^{199}) + C_{\mathrm{y}}(\mathrm{aq})(A_{199}^{202} A_{202}^{201} - A_{199}^{201} A_{202}^{202})}{R_1(A_{\mathrm{n}}^{202} A_{202}^{199} - A_{\mathrm{n}}^{199} A_{202}^{202}) + R_2(A_{\mathrm{n}}^{201} A_{202}^{201} - A_{\mathrm{n}}^{201} A_{202}^{202}) + (A_{\mathrm{n}}^{199} A_{202}^{202} - A_{\mathrm{n}}^{202} A_{202}^{199})} \quad (10)$$

The second key step of the proposed method is to calculate the amount of released Hg re-adsorbed on cinnabar ($C_{\mathrm{d}}(\mathrm{ads})$). Since the total amount of spiked ^{202}Hg ($C_{\mathrm{x}}(\mathrm{tot})$) is a known value, the amount of spiked ^{202}Hg adsorbed on cinnabar ($C_{\mathrm{x}}(\mathrm{ads})$) at each sampling time can be obtained by subtracting $C_{\mathrm{x}}(\mathrm{aq})$ from $C_{\mathrm{x}}(\mathrm{tot})$. If $C_{\mathrm{d}}(\mathrm{ads})$ can be related to $C_{\mathrm{x}}(\mathrm{ads})$, it would be feasible to calculate $C_{\mathrm{d}}(\mathrm{ads})$ by $C_{\mathrm{x}}(\mathrm{ads})$ and $C_{\mathrm{d}}(\mathrm{aq})$. Isotope ratios of Hg adsorbed on cinnabar surface are controlled by the adsorption/desorption process, while both adsorption/desorption and dissolution processes determine the ratios of Hg in the aqueous phase. As adsorption/desorption of Hg on cinnabar is expected to be much faster than cinnabar dissolution,[17] it is reasonable to assume that the isotope ratios of Hg in the aqueous phase is approximately equal to that adsorbed on cinnabar (Eq. (11)) due to the quick exchange of Hg isotopes between the aqueous and the particulate phases. This assumption was verified by the experiments described later.

$$\frac{C_{\mathrm{d}}(\mathrm{ads})}{C_{\mathrm{x}}(\mathrm{ads})} = \frac{C_{\mathrm{d}}(\mathrm{aq})}{C_{\mathrm{x}}(\mathrm{aq})} \quad (11)$$

By resolving Eq. (11), the amount of released Hg^{2+} that was re-adsorbed on cinnabar surface can be calculated from the released Hg in the aqueous phase and the distribution of spiked ^{202}Hg between the aqueous phase and cinnabar adsorbed phase using Eq. (12).

$$C_{\mathrm{d}}(\mathrm{ads}) = \frac{C_{\mathrm{x}}(\mathrm{tot}) - C_{\mathrm{x}}(\mathrm{aq})}{C_{\mathrm{x}}(\mathrm{aq})} C_{\mathrm{d}}(\mathrm{aq}) \quad (12)$$

Accordingly, the total amount of Hg released from cinnabar ($C_\mathrm{d}(\mathrm{tot})$) can be calculated by summing measured dissolved Hg in the aqueous phase ($C_\mathrm{d}(\mathrm{aq})$) and estimated Hg adsorbed on cinnabar surface ($C_\mathrm{d}(\mathrm{ads})$).

$$C_\mathrm{d}(\mathrm{tot}) = C_\mathrm{d}(\mathrm{aq}) + C_\mathrm{d}(\mathrm{ads}) = C_\mathrm{d}(\mathrm{aq}) + \frac{C_\mathrm{x}(\mathrm{tot}) - C_\mathrm{x}(\mathrm{aq})}{C_\mathrm{x}(\mathrm{aq})} C_\mathrm{d}(\mathrm{aq}) \qquad (13)$$

Application of the developed new technique in monitoring cinnabar dissolution and Hg^{2+} re-adsorption

The developed new technique was applied in determining concentrations of Hg re-adsorbed on cinnabar surface ($C_\mathrm{d}(\mathrm{ads})$) and total amount of Hg released from cinnabar ($C_\mathrm{d}(\mathrm{tot})$). The results showed that spiked $^{202}Hg^{2+}$ was adsorbed on cinnabar surface quickly under both oxic and anoxic conditions, illustrated by the rapid decrease in dissolved $^{202}Hg^{2+}$ concentrations in the first 6 hours (Fig. 2A and 2B). For the treatment of purging with N_2, the variation in both the released Hg present in the aqueous phase and total amount of released Hg was observed to be insignificant (p>0.1, one-way ANOVA) during the course of experiment (54 hours), indicating that dissolution of Hg from cinnabar was negligible under anaerobic condition. In the presence of O_2, detectable amount of Hg was dissolved from cinnabar, indicated by the continuous increase of both $C_\mathrm{d}(\mathrm{aq})$ and $C_\mathrm{d}(\mathrm{tot})$ with time (Fig. 2D). The concentration of total released Hg was estimated to be more than 300 μg L^{-1} after 54 hours. A number of previous studies also suggested that O_2 can enhance the dissolution of cinnabar.[10-13] Oxygen is expected to oxidize S^{2-} (one product of cinnabar dissolution) to SO_4^{2-}, and thus facilitating the dissolution of cinnabar.

As shown in Fig. 2A, natural Hg^{2+} in the solution was approximately 6 μg L^{-1} at the beginning of the experiment (0 hour), while the concentration for the control treatment (without the addition of $^{202}Hg^{2+}$) was approximately zero. The abnormal high concentration of natural Hg after the addition of $^{202}Hg^{2+}$ could be caused by the instant adsorption of spiked $^{202}Hg^{2+}$ on cinnabar and the subsequent replacement of natural Hg from cinnabar surface. Although cinnabar particles were cleaned for several times with 1 mol L^{-1} nitric acid and DI water prior to the experiment, there could be still some Hg ions adsorbed loosely on the surface. This assumption was further tested by measuring the replacement amount of Hg with different initial concentrations of $^{201}Hg^{2+}$ spiked. As shown in Fig. S3, the concentrations of Hg were less than 1 μg L^{-1} before $^{201}Hg^{2+}$ was spiked. An instant increase in Hg^{2+} was observed after the spike of $^{201}Hg^{2+}$ for all treatments. In addition, the concentration of natural Hg^{2+} increased gradually with the increasing concentration of spiked $^{201}Hg^{2+}$ (more $^{201}Hg^{2+}$ was instantly adsorbed on cinnabar). These results indicate that the initial increase of Hg concentration may be due to the isotopic replacement of residual adsorbed Hg on cinnabar with the spiked isotope-enriched Hg, rather than the cinnabar dissolution. Therefore, this Hg was deducted from the measured $C_{\mathrm{d}}(\mathrm{aq})$ when calculating the total released Hg from cinnabar ($C_{\mathrm{d}}(\mathrm{tot})$).

Importance of Hg re-adsorption on cinnabar dissolution estimation was evaluated by comparing the amount of released Hg from cinnabar with and without the consideration of the re-adsorption of released Hg on cinnabar. As shown in Fig. 2D, concentrations of total dissolved Hg were found to be much higher than that in the solution (~ 2 times), suggesting that a large proportion of released Hg from cinnabar was re-adsorbed on cinnabar surface. To further evaluate the importance of Hg re-adsorption on cinnabar dissolution, parameters relevant to the adsorption of Hg and the dissolution of cinnabar were calculated using Eq. (5) and Eq. (6). Variation of spiked ^{202}Hg fitted well with the pseudo-second order model, as indicated by the high value of R^2 (0.9999) (Fig. 3A). Dissolution of cinnabar could be well predicted by the first order reaction equation (R^2 = 0.9898, Fig. 3B).[34] Cinnabar dissolution rate constant was estimated to be 0.0208 h^{-1} when considering the re-adsorption of Hg on cinnabar surface by using the new method developed in this study (Table 1). If only dissolved Hg in the aqueous phase ($C_\mathrm{d}(\mathrm{aq})$) was taken into account, this rate constant would decrease to 0.0109 h^{-1} (Fig. 3C), indicating that ignoring the adsorption of Hg on cinnabar surface would significantly underestimate the dissolution rate of cinnabar.

Dissolution of cinnabar can serve as a continuous source for bioavailable Hg^{2+} in the environment, and subsequently facilitates the methylation process and increasing the amount of more toxic methylmercury. A number of previous studies have made efforts to quantify the importance of this process in the environment.[3, 6, 7, 10] Due to the lack of a feasible technique for measuring Hg adsorbed on cinnabar, only the Hg detected in the aqueous phase was considered to be dissolved from cinnabar in previous studies [11, 12] although several of which have speculated that dissolved Hg from cinnabar surface could be re-adsorbed on cinnabar surface.[10-12] A number of ligands are present in natural waters and they are expected to be involved in cinnabar dissolution by either affecting the release of Hg from cinnabar or adsorption of Hg on cinnabar surface via complexing with the dissolved Hg^{2+}.[6, 7] It should be noted that experiments in this study were conducted in a dilute $NaNO_3$ solution system without the addition of any inorganic or organic ligands. Future work of applying the developed method in determining cinnabar dissolution in natural waters would be helpful for better understanding the importance of cinnabar dissolution in Hg cycling.

Thermodynamics of Hg adsorption on cinnabar and Validation of the Hypothesis of the Proposed Method

Thermodynamics of Hg adsorption on cinnabar were further investigated by using the isotope-tracer method. As shown in Fig. 4A, percentage of ^{202}Hg adsorbed on cinnabar decreased from 94 to 48% with the increase of initial $^{202}Hg^{2+}$ concentration from 0 to 400 μg L^{-1}, while the equilibrium adsorption capacity increased from 94 to 1930 μg g^{-1}. At higher concentrations of initial Hg, adsorption sites on cinnabar may be over occupied which could explain the negative relation of Hg removal efficiency with initial Hg concentration.[40] The increasing equilibrium adsorption capacity at higher Hg concentrations could be attributed to the higher adsorption rate at higher concentration and the fully utilization of available active sites.[28] Nonlinear regression of the equilibrium adsorption capacity q_e (μg g^{-1}) against the equilibrium concentration of $^{202}Hg^{2+}$ C_e (μg L^{-1}) using both Langmuir and Freundlich models were conducted to estimate the relevant parameters of adsorption. Langmuir model predicted the experimental data better than Freundlich model, indicating by its higher R^2 (Table 1, and Fig. 4B).

In order to derive the equation for calculating the total released Hg ($C_{\mathrm{d}}(\mathrm{tot})$), it was assumed that the isotope ratio of Hg in the solution was identical with that adsorbed on cinnabar (Eq. (11)). This assumption was formulated based partially on that rates of Hg adsorption/desorption were much higher than cinnabar dissolution. As shown in Fig. 2B and 2D, the dissolution of cinnabar has not achieved equilibrium at the end of the experiments (54 hours), while the equilibrium time for Hg adsorption was determined to be less than 6 hours, supporting this assumption. In order to further verify the hypothesis, concentrations of dissolved Hg in the solution $C_{\mathrm{d}}(\mathrm{tot})$ were also calculated based on the thermodynamic model (Langmuir model). Total Hg ions detected at t time can be considered as C_e (i.e. C_d(aq) + C_x(aq)). Parameters (K_L and q_m) obtained from the thermodynamic experiments in the presence of N_2 were adopted. By using Langmuir model, total adsorbed Hg on cinnabar can be calculated (Eq. (1&2)) as $C_{\mathrm{d+x}}(\mathrm{ads})$. Then, the total amount of dissolved Hg can be estimated as:

$$C_{\mathrm{d}}(\mathrm{tot}) = C_{\mathrm{d}}(\mathrm{aq}) + C_{\mathrm{d}}(\mathrm{ads}) = C_{\mathrm{d}}(\mathrm{aq}) + (C_{\mathrm{d+x}}(\mathrm{ads}) - C_{\mathrm{x}}(\mathrm{ads})) \qquad (14)$$

The comparisons of total dissolved Hg calculated by both methods were shown in Fig. 5. Total dissolved Hg estimated by Langmuir model (Eq. (14)) was observed to be higher than that estimated using the newly developed method at the first 6 hours and then became very close in the presence of O_2 (Fig. 5B). This is reasonable since the adsorption of spiked Hg had not achieved equilibrium at the beginning of the experiment and was expected to result in the overestimation of Hg adsorbed on cinnabar if Langmuir model was adopted. Dissolved Hg estimated using both methods were observed to be similar (p>0.05, two-way ANOVA), especially after 6 hours (p>0.1, two-way ANOVA, with an average RSD of 9.9% (2.4-16.6%) when Hg in the aqueous phase and cinnabar surface was expected to be equilibrated. These results further support the hypothesis that the isotope ratio of Hg in the solution is approximately identical with that adsorbed on cinnabar, suggesting the reliability of the proposed method in estimating the real dissolution of cinnabar. On basis of these validations, the errors originated from the assumption should be reasonable and the proposed method is expected to be a reliable technique in studying the dissolution of cinnabar.

ENVIRONMENTAL IMPLICATION

In this study, an isotope tracer based method was developed to investigate both dissolution and re-adsorption of Hg during the course of cinnabar dissolution. By using this method, re-adsorption of Hg on cinnabar surface was found to play an important role in accurately evaluating cinnabar dissolution, and the rates of cinnabar dissolution could be significantly underestimated without considering the re-adsorption process. Cinnabar dissolution is deemed to be an important factor in Hg cycling as this process could serve as a continuous source for reactive Hg in aquatic environments, increasing the possibility of Hg transport, methylation and bioaccumulation in aquatic environments. Results of this study suggest that the re-adsorption of released Hg on cinnabar surface is more important than previously expected in Hg cycling and this process should be taken into account in future studies of cinnabar dissolution.

SUPPORTING INFORMATION

Additional information as noted in the text. This material is available free of charge via the internet at http://pubs.acs.org

ACKNOWLEDGEMENT

This research was partially supported by the National Basic Research Program of China (2013CB430002), National Natural Science Foundation of China (21120102040, 21577134), and US Department of Energy (DE-FG01-05EW07033). This is contribution number XXX of the Southeast Environmental Research Center at Florida International University.

REFERENCE

(1) Barnett, M. O.; Harris, L. A.; Turner, R. R.; Stevenson, R. J.; Henson, T. J.; Melton, R. C.; Hoffman, D. P., Formation of mercuric sulfide in soil. *Environ. Sci. Technol.* **1997,** *31*, 3037-3043.

(2) Benoit, J. M.; Gilmour, C. C.; Mason, R. P.; Heyes, A., Sulfide controls on mercury speciation and bioavailability to methylating bacteria in sediment pore waters. *Environ. Sci. Technol.* **1999,** *33*, 951-957.

(3) Burkstaller, J. E.; McCarty, P. L.; Parks, G. A., Oxidation of cinnabar by iron(III) in acid mine waters. *Environ. Sci. Technol.* **1975,** *9*, 676-678.

(4) Paquette, K.; Helz, G., Solubility of cinnabar(red HgS) and implications for mercury speciation sulfidic waters. *Water Air Soil Pollut.* **1995,** *80*, 1053-1056.

(5) Ravichandran, M.; Aiken, G. R.; Reddy, M. M.; Ryan, J. N., Enhanced dissolution of cinnabar (mercuric sulfide) by aquatic humic substances. *ABSTR PAP AM CHEM S* **1998,** *216*, U785-U785.

(6) Ravichandran, M.; Aiken, G. R.; Reddy, M. M.; Ryan, J. N., Enhanced dissolution of cinnabar (mercuric sulfide) by dissolved organic matter isolated from the Florida Everglades. *Environ. Sci. Technol.* **1998,** *32*, 3305-3311.

(7) Waples, J. S.; Nagy, K. L.; Aiken, G. R.; Ryan, J. N., Dissolution of cinnabar (HgS) in the presence of natural organic matter. *Geochim. Cosmochim. Acta* **2005,** *69*, 1575-1588.

(8) Liu, G.; Cabrera, J.; Allen, M.; Cai, Y., Mercury characterization in a soil sample collected nearby the DOE Oak Ridge Reservation utilizing sequential extraction and thermal desorption method. *Sci. Total Environ.* **2006,** *369*, 384-392.

(9) Ravichandran, M., Interactions between mercury and dissolved organic matter - a review. *Chemosphere* **2004,** *55*, 319-331.

(10) Barnett, M. O.; Turner, R. R.; Singer, P. C., Oxidative dissolution of metacinnabar (beta-HgS) by dissolved oxygen. *Appl. Geochem.* **2001,** *16*, 1499-1512.

(11) Holley, E. A.; McQuillan, A. J.; Craw, D.; Kim, J. P.; Sander, S. G., Mercury mobilization by oxidative dissolution of cinnabar (alpha-HgS) and metacinnabar (beta-HgS). *Chem. Geol.* **2007,** *240*, 313-325.

(12) He, Z.; Traina, S. J.; Weavers, L. K., Sonochemical Dissolution of Cinnabar (α-HgS). *Environ. Sci. Technol.* **2007,** *41*, 773-778.

(13) Hsieh, Y. H.; Tokunaga, S.; Huang, C. P., Some chemical reactions at the HgS(s)—water interface as affected by photoirradiation. *Colloids Surf.* **1991,** *53*, 257-274.

(14) Aiken, G. W., J.; Nagy, K. L.; Ryan, J.; Ravichandran, M., Dissolution of cinnabar by dissolved organic matter. *ABSTR PAP AM CHEM S* **2001,** *222*, U425-U425.

(15) Gu, B.; Bian, Y.; Miller, C. L.; Dong, W.; Jiang, X.; Liang, L., Mercury reduction and complexation by natural organic matter in anoxic environments. *Proc. Natl. Acad. Sci. U. S. A.* **2011,** *108*, 1479-1483.

(16) Lockwood, R. A.; Chen, K. Y., Adsorption of mercury(II) by hydrous manganese oxides. *Environ. Sci. Technol.* **1973,** *7*, 1028-1034.

(17) Yin, Y.; Allen, H. E.; Huang, C. P.; Sparks, D. L.; Sanders, P. F., Kinetics of Mercury(II) Adsorption and Desorption on Soil. *Environ. Sci. Technol.* **1997,** *31*, 496-503.

(18) Hintelmann, H.; Harris, R., Application of multiple stable mercury isotopes to determine the adsorption and desorption dynamics of Hg(II) and MeHg to sediments. *Mar. Chem.* **2004,** *90*, 165-173.

(19) Miretzky, P.; Bisinoti, M. C.; Jardim, W. F.; Rocha, J. C., Factors affecting Hg (II) adsorption in soils from the Rio Negro basin (Amazon). *Quim. Nova* **2005,** *28*, 438-443.

(20) Bonnissel-Gissinger, P.; Alnot, M.; Lickes, J.-P.; Ehrhardt, J.-J.; Behra, P., Modeling the Adsorption of Mercury(II) on (Hydr)oxides II: α-FeOOH (Goethite) and Amorphous Silica. *J. Colloid Interface Sci.* **1999,** *215*, 313-322.

(21) Balsley, S. D.; Brady, P. V.; Krumhansl, J. L.; Anderson, H. L., Iodide Retention by Metal Sulfide Surfaces: Cinnabar and Chalcocite. *Environ. Sci. Technol.* **1996,** *30*, 3025-3027.

(22) Schuster, E., The behavior of mercury in the soil with special emphasis on complexation and adsorption processes - A review of the literature. *Water Air Soil Pollut.* **1991,** *56*, 667-680.

(23) Li, Y.; Mao, Y.; Liu, G.; Tachiev, G.; Roelant, D.; Feng, X.; Cai, Y., Degradation of Methylmercury and Its Effects on Mercury Distribution and Cycling in the Florida Everglades. *Environ. Sci. Technol.* **2010,** *44*, 6661-6666.

(24) Li, Y.; Yin, Y.; Liu, G.; Tachiev, G.; Roelant, D.; Jiang, G.; Cai, Y., Estimation of the Major Source and Sink of Methylmercury in the Florida Everglades. *Environ. Sci. Technol.* **2012,** *46*, 5885-5893.

(25) Mann, J. L.; Long, S. E.; Kelly, W. R., Direct determination of mercury at picomole L-1 levels in bottled water by isotope dilution cold-vapor generation inductively coupled plasma mass spectrometry. *J. Anal. At. Spectrom.* **2003,** *18*, 1293-1296.

(26) Freundlich, H., Over the Adsorption in Solution. *J. Phys. Chem.* **1906,** *57*, 385-471.

(27) Langmuir, I., The adsorption of gases on plane surfaces of glass, mica and platinum. *JACS* **1918,** *40*, 1361-1403.

(28) Senthil Kumar, P.; Senthamarai, C.; Durgadevi, A., Adsorption kinetics, mechanism, isotherm, and thermodynamic analysis of copper ions onto the surface modified agricultural waste. *Environ Prog Sustain Energy* **2014,** *33*, 28-37.

(29) Farooq, U.; Kozinski, J. A.; Khan, M. A.; Athar, M., Biosorption of heavy metal ions using wheat based biosorbents – A review of the recent literature. *Bioresour. Technol.* **2010,** *101*, 5043-5053.

(30) Kołodyńska, D.; Wnętrzak, R.; Leahy, J. J.; Hayes, M. H. B.; Kwapiński, W.; Hubicki, Z., Kinetic and adsorptive characterization of biochar in metal ions removal. *Chem. Eng. J.* **2012,** *197*, 295-305.

(31) Hasany, S. M.; Chaudhary, M. H., Sorption potential of Haro river sand for the removal of antimony from acidic aqueous solution. *Appl. Radiat. Isot.* **1996,** *47*, 467-471.

(32) Lazaridis, N. K.; Asouhidou, D. D., Kinetics of sorptive removal of chromium(VI) from aqueous solutions by calcined Mg–Al–CO3 hydrotalcite. *Water Res.* **2003,** *37*, 2875-2882.

(33) Ho, Y. S.; McKay, G., Pseudo-second order model for sorption processes. *Process Biochem.* **1999,** *34*, 451-465.

(34) M. Sut, T. F., F. Repmann and T. Raab, Long-Term Release of Iron-Cyanide Complexes from the Soils of a Manufactured Gas Plant Site. *Journal of Environmental Protection* **2013,** *4*, 8-19.

(35) Long, S. E.; Kelly, W. R., Determination of Mercury in Coal by Isotope Dilution Cold-Vapor Generation Inductively Coupled Plasma Mass Spectrometry. *Anal. Chem.* **2002,** *74*, 1477-1483.

(36) Heumann, K. G.; Gallus, S. M.; Rädlinger, G.; Vogl, J., Accurate determination of element species by on-line coupling of chromatographic systems with ICP-MS using isotope dilution technique. *Spectrochim. Acta, Part B* **1998,** *53*, 273-287.

(37) Hintelmann, H.; Evans, R. D., Application of stable isotopes in environmental tracer studies – Measurement of monomethylmercury (CH3Hg+) by isotope dilution ICP-MS and detection of species transformation. *Fresenius. J. Anal. Chem.* **1997,** *358*, 378-385.

(38) Rodríguez-González, P.; Marchante-Gayón, J. M.; García Alonso, J. I.; Sanz-Medel, A., Isotope dilution analysis for elemental speciation: a tutorial review. *Spectrochim. Acta, Part B* **2005,** *60*, 151-207.

(39) Smith, R. G., Determination of mercury in environmental samples by isotope dilution/ICPMS. *Anal. Chem.* **1993,** *65*, 2485-2488.

(40) Javadian, H.; Ghaemy, M.; Taghavi, M., Adsorption kinetics, isotherm, and thermodynamics of Hg2+ to polyaniline/hexagonal mesoporous silica nanocomposite in water/wastewater. *J. Mater. Sci.* **2014,** *49*, 232-242.

Figure legends

Figure 1 A schematic showing the procedure of simultaneously monitoring the dissolution of cinnabar and re-adsorption of released Hg using isotope tracer and isotope dilution techniques.

Figure 2. Variations of spiked $^{202}Hg^{2+}$ in aqueous phase ($C_X(\mathrm{aq})$), Hg dissolved from cinnabar in aqueous phase ($C_\mathrm{d}(\mathrm{aq})$), and the total Hg dissolved from cinnabar ($C_\mathrm{d}(\mathrm{tot})$). A and C, purging with N_2; B and D, purging with O_2. Since $C_\mathrm{d}(\mathrm{aq})$ at time 0 was likely resulted from the isotopic replacement of natural Hg adsorbed on cinnabar by the spiked $^{202}Hg^{2+}$, rather than the cinnabar dissolution, this Hg was deducted from the measured $C_\mathrm{d}(\mathrm{aq})$ when calculating the total released Hg from cinnabar ($C_\mathrm{d}(\mathrm{tot})$).

Figure 3. Nonlinear regressions of spiked ^{202}Hg (A), total dissolved Hg (B), and dissolved Hg in the aqueous phase (C) against time.

Figure 4. The thermodynamic of $^{202}Hg^{2+}$ adsorption on cinnabar. A, variation of equilibrium concentrations of ^{202}Hg (μg L^{-1}) at 24 h with different initial $^{202}Hg^{2+}$ concentrations (0, 10, 20, 50, 100, 200, 400 μg L^{-1}). B, non-linear regression of q_e against C_e using Langmuir and Freundlich models (T = 20 °C).

Figure 5. Comparisons of total dissolved Hg estimated by the thermodynamic equilibrium using Langmur model (eq.14) and by the new method developed in this study (eq.13). A, without O_2 (purging with N_2); B, with O_2 (purging with O_2).

Figure 1

$^{N}Hg^{2+}$(aq) is the released Hg from cinnabar present in the aqueous phase.
$^{N}Hg^{2+}$(ads) is the released Hg re-adsorbed on cinnabar surface.
$^{202}Hg^{2+}$ (aq) is spiked $^{202}Hg^{2+}$ present in the aqueous phase.
$^{202}Hg^{2+}$ +(ads) is spiked $^{202}Hg^{2+}$ adsorbed on cinnabar surface.

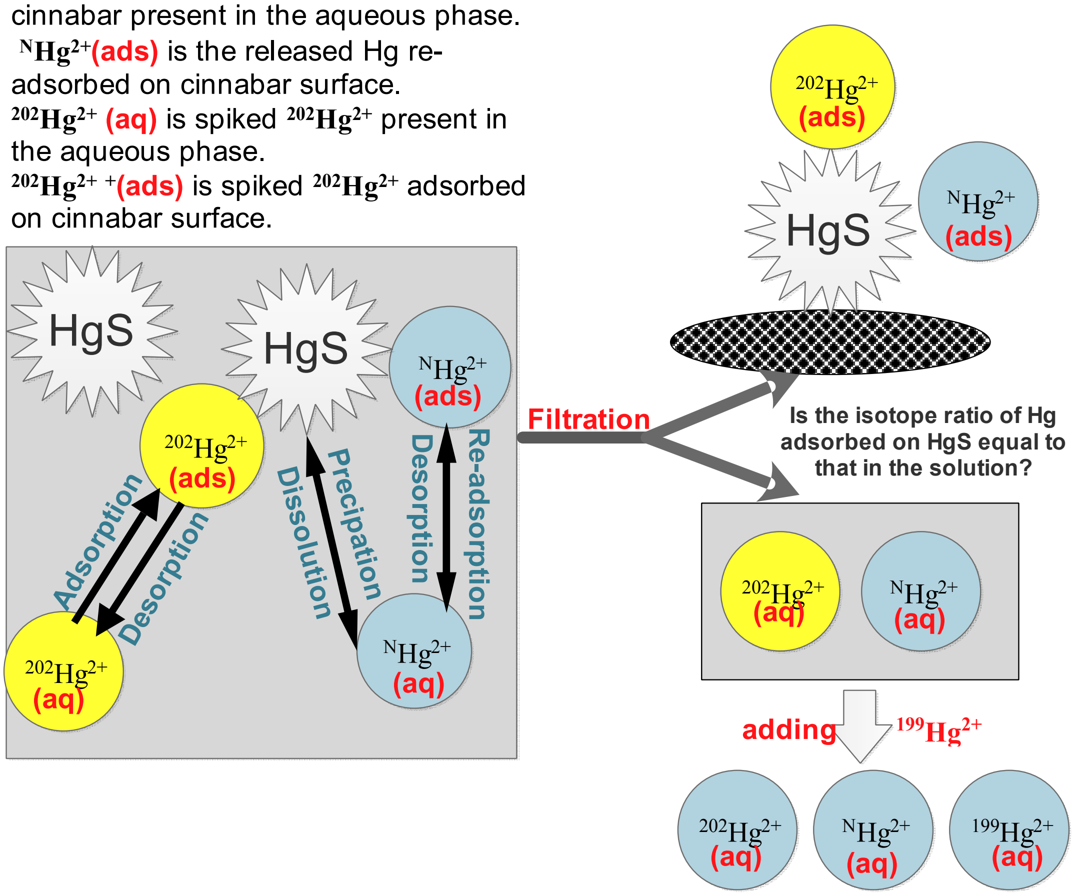

Figure 2

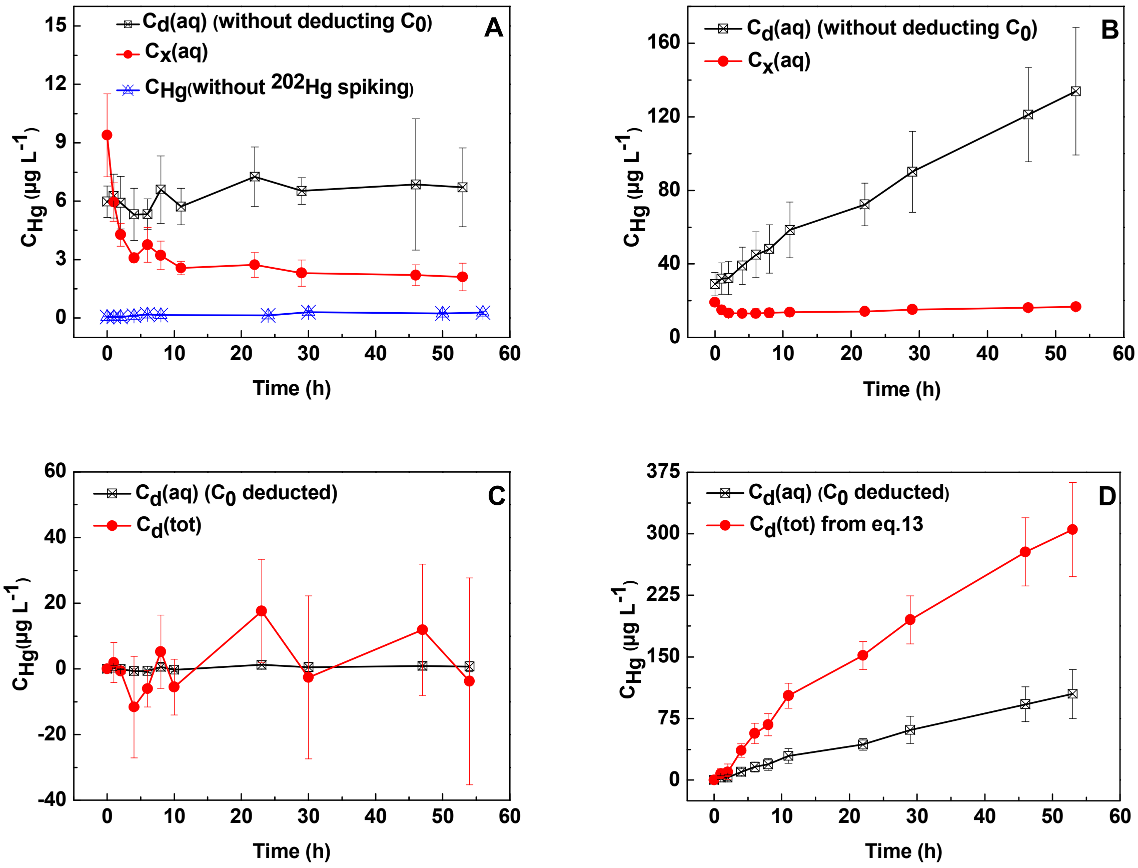
A
Cd(aq) (without deducting C0)
Cx(aq)
CHg(without 202Hg spiking)
CHg (μg L-1)
Time (h)
B
Cd(aq) (without deducting C0)
Cx(aq)
CHg (μg L-1)
Time (h)
C
Cd(aq) (C0 deducted)
Cd(tot)
CHg(μg L-1)
Time (h)
D
Cd(aq) (C0 deducted)
Cd(tot) from eq.13
CHg (μg L-1)
Time (h)

Figure 3

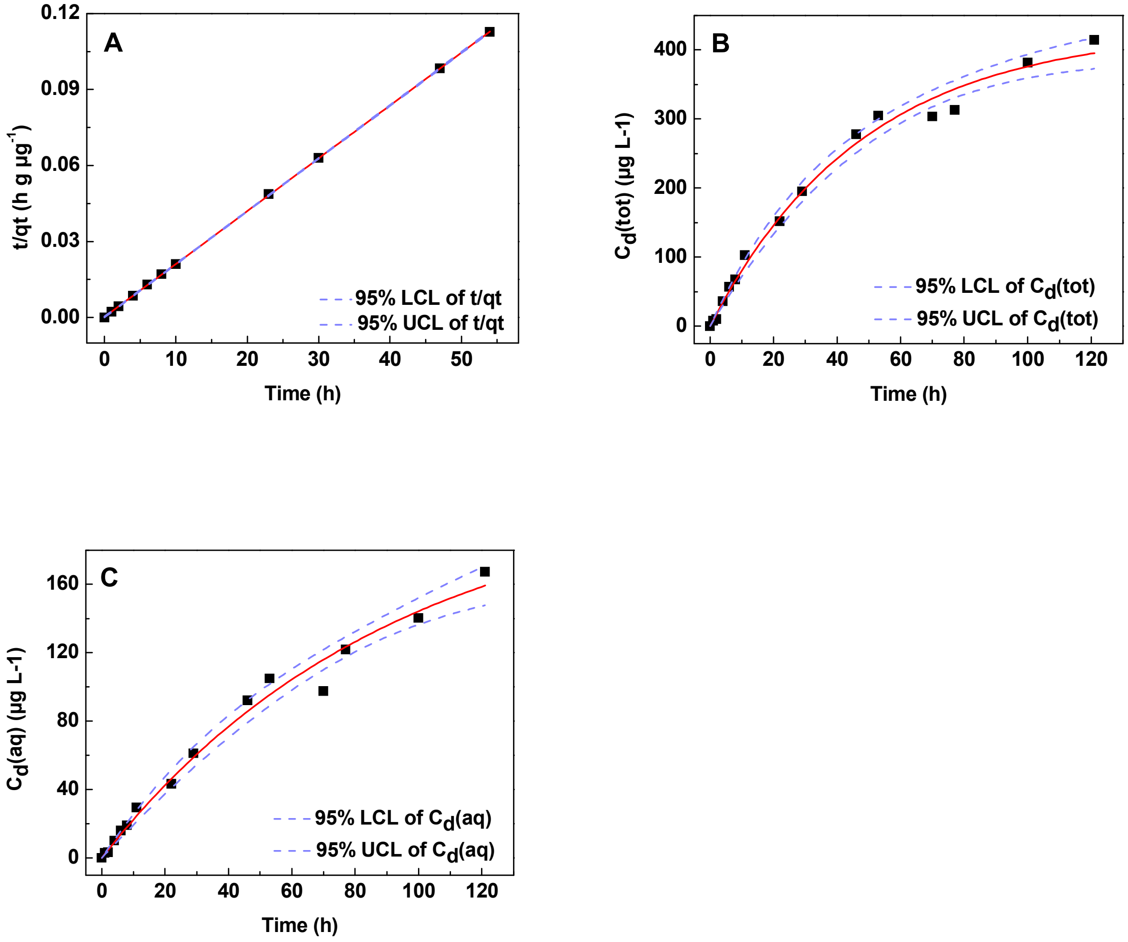
A
t/qt (h g μg^{-1})
0.12
0.09
0.06
0.03
0.00
0
10
20
30
40
50
Time (h)
95% LCL of t/qt
95% UCL of t/qt
B
C_d(tot) (μg L-1)
400
300
200
100
0
0
20
40
60
80
100
120
Time (h)
95% LCL of C_d(tot)
95% UCL of C_d(tot)
C
C_d(aq) (μg L-1)
160
120
80
40
0
0
20
40
60
80
100
120
Time (h)
95% LCL of C_d(aq)
95% UCL of C_d(aq)

Figure 4

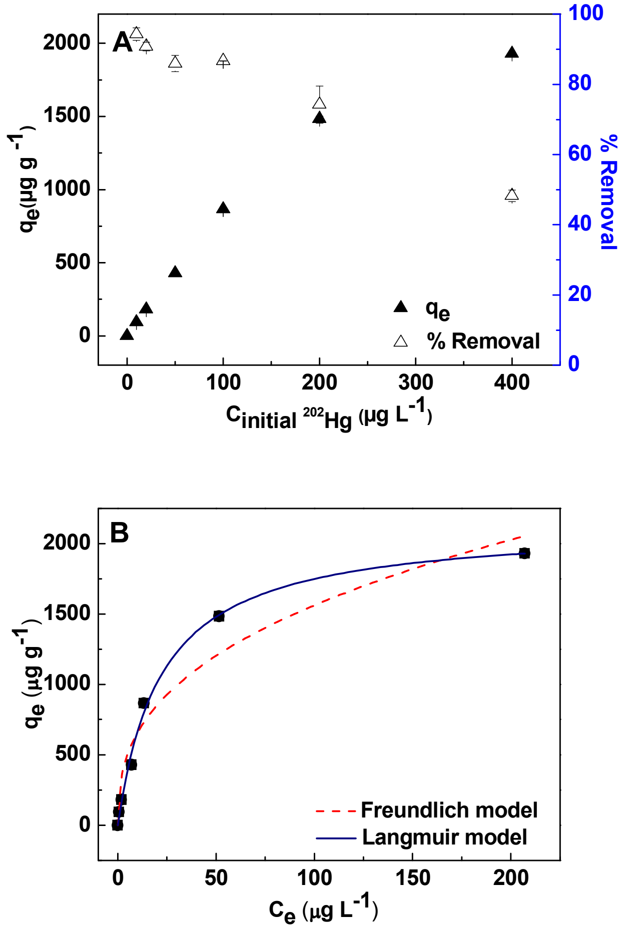
A
q_e (μg g^{-1})
2000
1500
1000
500
0
100
80
60
40
20
0
% Removal
▲ q_e
△ % Removal
0
100
200
300
400
$C_{initial}$ ^{202}Hg (μg L^{-1})
B
q_e (μg g^{-1})
2000
1500
1000
500
0
Freundlich model
Langmuir model
0
50
100
150
200
C_e (μg L^{-1})

Figure 5

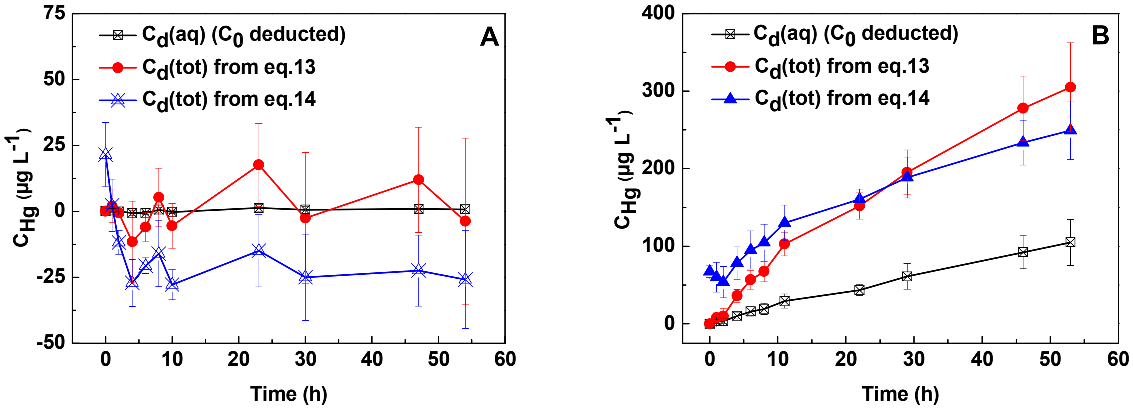
A
C_d(aq) (C_0 deducted)
C_d(tot) from eq.13
C_d(tot) from eq.14
C_{Hg} (µg L^{-1})
75
50
25
0
-25
-50
0
10
20
30
40
50
60
Time (h)
B
C_d(aq) (C_0 deducted)
C_d(tot) from eq.13
C_d(tot) from eq.14
C_{Hg} (µg L^{-1})
400
300
200
100
0
0
10
20
30
40
50
60
Time (h)

Table 1 Parameters of adsorption kinetics and isotherms of Hg on cinnabar using different models (in the absence of O_2) and dissolution (in the present of O_2)

Kinetic models	Parameters	Values	R^2
The pseudo-second order rate equation	q_e (μg g^{-1})	485.4	0.9999
$\frac{dq_t}{dt} = k_1(q_e - q_t)^2$ $\frac{t}{q_t} = \frac{1}{K_2 q_e{}^2} + \frac{1}{q_e} t$	K_2 (g μg^{-1}h^{-1})	0.00663	
Dissolution kinetic model	C_0 (tot)(μg L^{-1})	430.26	0.9898
$C = C_0 . (1 - e^{-kt})$	K (tot)(hour^{-1})	0.0208	
	C_0 (aq)(μg L^{-1})	217.55	0.9851
	K (aq) (hour^{-1})	0.0109	
Langmuir model	q_m (μg g^{-1})	2137.1	0.9952
$q_e = \frac{q_m k_L C_e}{1 + k_L C_e}$	K_L (L μg^{-1})	0.0450	
Freundlich model	K_F (μg g^{-1})	275.89	0.9390
$q_e = K_F C_e^{1/n}$	1/n (g L^{-1})	0.375	